

# CHARACTERIZATION OF MICROSTRUCTURE AND TEXTURE OF A TITANIUM ALLOY CORONA 5

S. BENHADDAD, C. QUESNE and R. PENELLE

*Laboratoire de Métallurgie Structurale U.R.A CNRS 1107,  
Bât 413 Université Paris-Sud, 91405 Orsay Cedex France*

*(Received 29 July 1994)*

Both parameters, microstructure and texture, are studied on several samples for different processes. The same route, thermomechanical treatment (forging or rolling) followed by solutioning and ageing is carried out with various temperature and deformation amount on an identical titanium alloy CORONA 5.

According to three temperature fields: low ( $\alpha + \beta$ ),  $\beta$  and high ( $\alpha + \beta$ ) three important microstructures are obtained: equiaxed, acicular and bimodal.

All measured textures present two components which vary with deformation mode and temperature of both forging and solutioning.

KEY WORDS: CORONA 5, microstructure, texture component.

## INTRODUCTION

The CORONA 5 is an ( $\alpha/\beta$ ) titanium alloy interesting for aerospace and naval applications because of a good combination of a corrosion resistance in chlorinated environment, a long fatigue life and a high fracture toughness.

It is well known that mechanical properties of titanium alloys are very sensitive to variations in microstructure and texture which depend on thermomechanical and heat treatments (Wanhill 1978, Bowen 1988).

The present paper deals with the characterization of the evolution of both microstructure and texture according to different routes.

## MATERIAL AND EXPERIMENTAL PROCEDURES

The CORONA 5 alloy (Ti-4.5Al-5Mo-1.5Cr weight %) was transformed by CEZUS. From an identical initial microstructure eight routes consisting of a forging or rolling followed by a solutioning treatment, all the structures have undergone the same ageing treatment, Table 1 (Benhaddad 1992).

**Table 1** Routes of treatments.

<i>deformation type</i>	<i>field</i>	<i>deformation amount</i>	<i>solutioning treatment</i>		<i>process name</i>
Rolling	$\beta$	—	$\alpha\beta$ high		R
Cross rolling	$\beta$	—	$\alpha\beta$ high	Ageing	CR
Forging	$\alpha\beta$ low	low	$\alpha\beta$ low		A
			process 1	—	1
Forging	$\alpha\beta$ high	high	$\alpha\beta$ high $\alpha\beta$ low	Treatment	B C
			process 2	—	2
Forging	$\beta$	high low	$\alpha\beta$ high $\alpha\beta$ low $\alpha\beta$ high		D E F

For metallographic studies the samples were cut perpendicularly to the bar axis D and electropolished using an electrolyte of 30 cm<sup>3</sup> perchloric acid + 175 cm<sup>3</sup> *n* butanol + 300 cm<sup>3</sup> methanol at -40°C and 24V. Then samples were etched in a solution of 2 cm<sup>3</sup> hydrofluoric acid, 3 cm<sup>3</sup> nitric acid + 95 cm<sup>3</sup> water.

The pole figures {0002}, {1010} and {1012} were measured by X-ray diffraction in reflection, in the case of the sample F having coarse grains, the pole figures were measured by neutron diffraction in transmission at laboratoire L. Brillouin in Saclay. The orientation distribution function (O.D.F) was calculated using Roe notation (Roe 1965). This function describes quantitatively the texture:

$$dV/V_0 = K.F(g).dg \quad (1)$$

$V_0$ : sample volume (orientation volume)

$K$ : normalization constant

and  $F(g)$ : orientation distribution function (O.D.F).

The function  $F(g)$  is calculated from four poles figures. The pole density  $q(\kappa, \eta)$  at a given point of a {hkil} pole figure is related to O.D.F by:

$$q(\kappa, \eta) = \frac{1}{2\pi} \int_0^{2\pi} F(g) d\gamma \quad (2)$$

$\kappa$  and  $\eta$ : spherical coordinates of the normal to diffracting plane in the specimen frame.

$d\gamma$ : rotation around the normal to the diffracting plane.

The O.D.F is calculated by inverting this integral, the principle of the calculation consists in expanding each member of this equation (2) on spherical harmonics basis and finding relations between the coefficients of both expansions (Bunge 1969).

The  $F(g)$  maximums represent the orientation density of the different components present in the studied polycrystal. Therefore, the texture can be represented by the preferential orientations with their respective  $F(g)$ .

## RESULTS AND DISCUSSION

### *Microstructure*

The microstructure is governed by:

- the forging temperature
- the deformation amount
- the solutioning temperature

\*According to the forging temperature, three kinds of  $\alpha$  phase morphology are observed (Figure 1):

- the equiaxed or globular morphology is obtained by forging in the  $(\alpha + \beta)$  field, route A.
- the acicular microstructure is obtained after forging in the  $\beta$  field, the  $\alpha$  phase precipitates at prior  $\beta$  grain boundaries and in the  $\beta$  matrix, routes D, E and F. The acicular structure is also observed after rolling in the  $\beta$  field, routes R and CR.
- the bimodal microstructure is obtained after forging in the  $(\alpha + \beta)$  field near the  $\beta$  transus.

\*The deformation amount acts upon the structure of the D and the F process. A high degree of deformation, D, leads to:

- a decrease of prior  $\beta$  grain size.
- a broken morphology of prior  $\beta$  grain.
- an increase of the number of needles  $\alpha$ .

\*The solutioning treatment in high  $\alpha/\beta$  field (B) leads to a small amount of the  $\beta$  stable phase, contrary to a treatment at lower temperature (C) after cooling. The  $\beta$  metastable phase is transformed in  $\alpha/\beta$  acicular.

### *Texture*

The texture is represented by the principal orientations  $\{hkil\} \langle uvw \rangle$ :  $\{hkil\}$  is the crystallographic plane parallel to the reference plane (T, N) and  $\langle uvw \rangle$  the crystallographic direction parallel to the transverse direction T, N is the perpendicular axis to the bar axis D (Figure 2). The  $\{0002\}$  pole figures are shown (Figure 3).

All the  $\{0002\}$  pole figures exhibit similar location of the maximum in the form of a cross in the principal planes (T, N) and (D, N) with sometimes a reinforcement at the center of the pole figure. The texture presents a mixed character with two components  $C_{DN}$  and  $C_{DT}$ . The component  $C_{DN}$  corresponds to basal planes with their axes  $\langle 0001 \rangle$  in the (D, N) plane. The second component  $C_{DT}$  corresponds to basal planes with their axis  $\langle 0001 \rangle$  in the (T, N) plane (Figure 4).

The  $F(g)_{max}$  of these two components varies with the temperature, the forging amount, and the temperature of solutioning treatment.

All  $C_{DN}$  and  $C_{DT}$  components, their intensity  $F(g)_{max}$  and their corresponding angle  $\gamma$  (angle between axes  $\langle 0001 \rangle$  of each component and the D axis) are given in the Table 2.

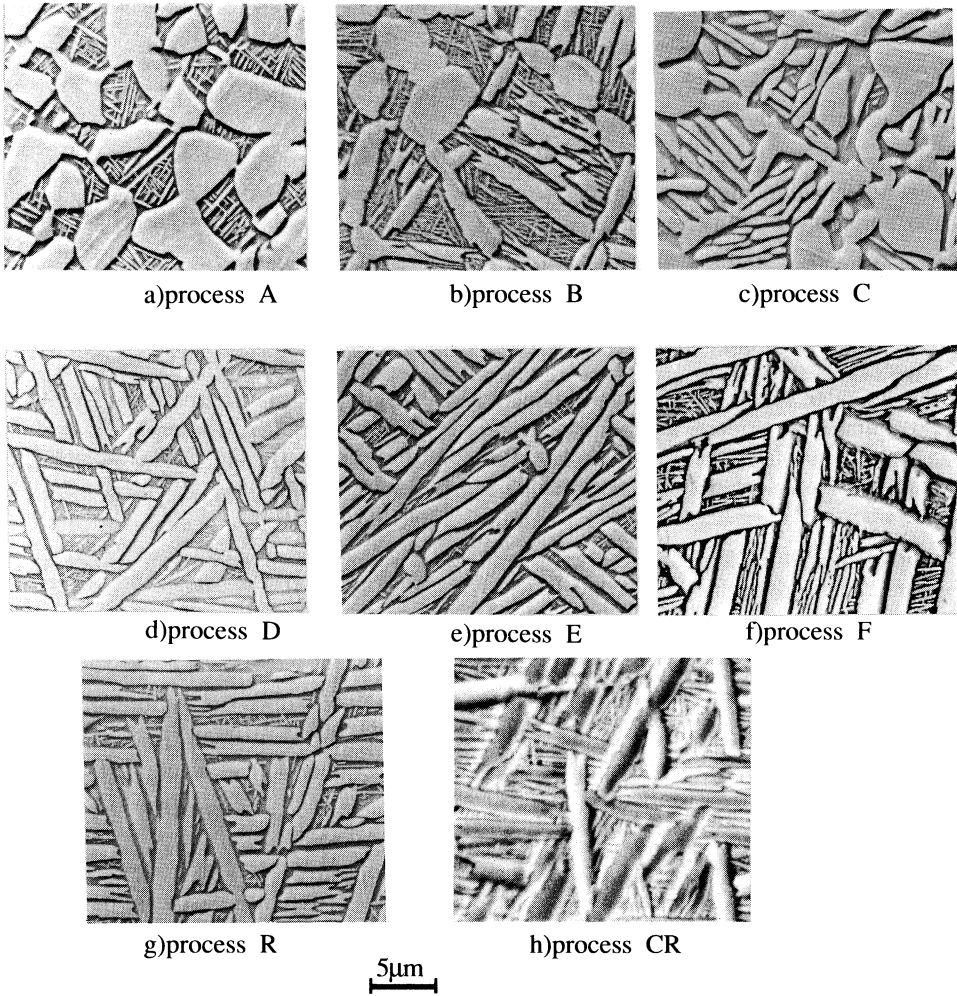


**Figure 1** Microstructure of the different samples.

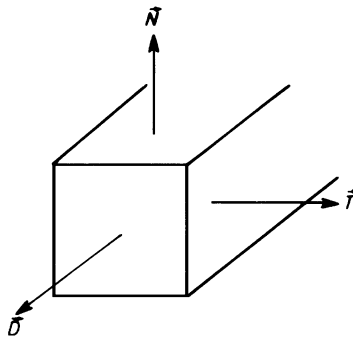


**Figure 2** The forging bar reference.

D: forging bar axis

N: normal axis

T: transverse axis

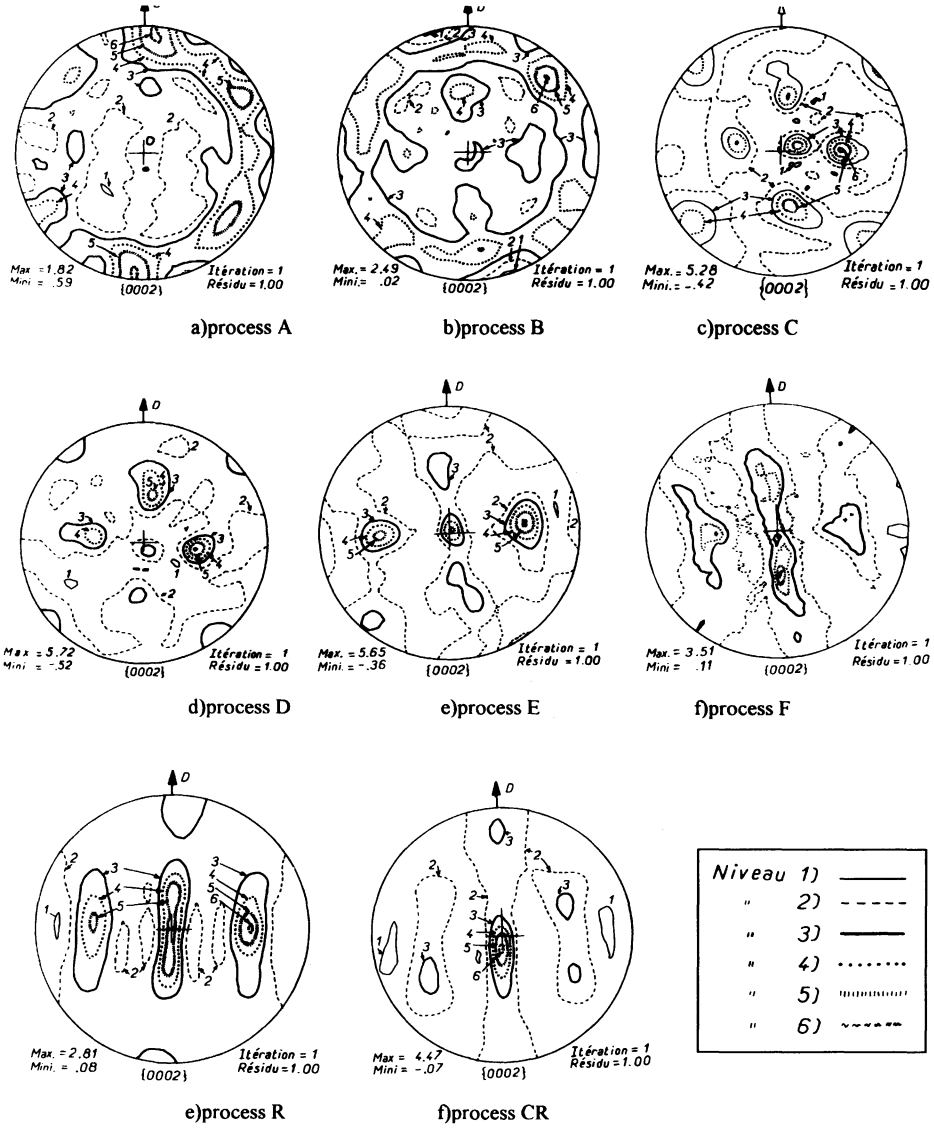


Figure 3 The recalculated pole figures.

*Effect of deformation mode*

For a same temperature different types of texture are obtained after each deformation mode. A cross rolling (CR) in the  $\beta$  phase field leads to a basal texture. On the contrary, the forging (F) or the unidirectional rolling (R) leads to two components near to the basal/transverse texture type (Peters *et al.*, 1980).

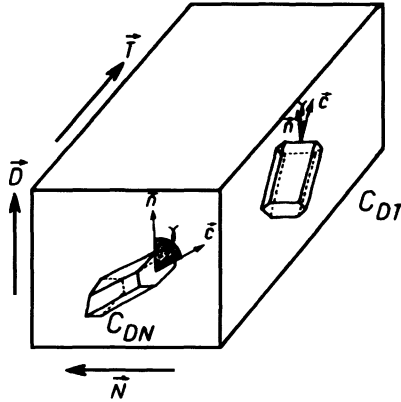


Figure 4 The texture components.

### Effect of solutioning temperature

For a same temperature and amount of, (process 1 or 2) the solutioning treatment at low temperature (process C or E) does not change the texture. However the solutioning treatment at high temperature in the  $(\alpha + \beta)$  phase field (process B or D) transforms the texture. The evolution of texture after a high solutioning treatment is:

- the axes  $c$  of the component  $C_{DN}$  are near to the deformation axis  $D$ .
- the axes  $c$  of the component  $C_{DT}$  are near to the transverse direction  $T$ .

### Effect of forging temperature

The Figures 5a and b exhibit evolution of  $C_{DN}$  and  $C_{DT}$  intensity as a function of forging temperature. The results are separated in "high treated" and "low treated". The same evolution is observed for the two classes:

- at high temperature, the intensity of  $C_{DN}$  is equal or lightly greater than the  $C_{DT}$  intensity.
- at low forging temperature (process A), the  $C_{DN}$  component is preponderant.

Table 2 Texture results.

Process	$C_{DT}$	$\gamma(^{\circ})$	$F(g)max$	$C_{DN}$	$\gamma(^{\circ})$	$F(g)max$
R	{1103}<2201>	32	3.20	{2112}<0110>	60	3.30
CR	—	—	—	{0001}<1010>	0	6.10
A	{2021}<1013>	78	3.00	—	—	—
1	{2023}<1011>	50	—	{2023}<1210>	50	—
B	{3032}<1013>	68	3.30	{1012}<1210>	42	2.20
C	{2023}<1011>	50	7.10	{2023}<1210>	50	8.50
2	{0001}<1210>	0	—	{1011}<1210>	60	—
D	{1012}<1011>	42	8.90	{1012}<1210>	42	10.60
E	{0001}<1120>	0	6.00	{1011}<1210>	60	8.10
F	{1103}<2201>	32	3.50	{1101}<1120>	60	3.20

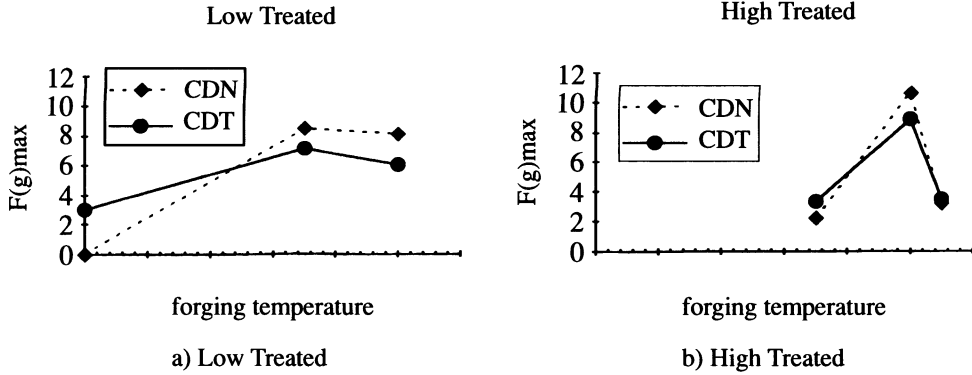


**Figure 5** Evolution of O.D.F as function of forging temperature.

The low intensity of texture of the sample F is essentially due to a decrease of the deformation amount of the F process comparatively to the D process.

The evolution of angle  $\gamma$ , between the axes  $\langle 0001 \rangle$  of each component and the deformation axis D, with the forging temperature is plotted Figures 6a and b.

It can be noted that:

- the angle  $\gamma$  of the  $C_{DN}$  component increases with forging temperature.
- the angle  $\gamma$  of the  $C_{DT}$  component decreases when the forging temperature is increased.

The tendency is the formation of transverse texture  $\{1010\} \langle 1210 \rangle$  at high temperature with eventually a component of basal texture  $\{0001\} \langle uvw \rangle$ .

*Comparative Evolution of Microstructure and Texture*

The evolution of both microstructure and texture with different processes shows that it is possible to obtain several combinations of these two parameters:

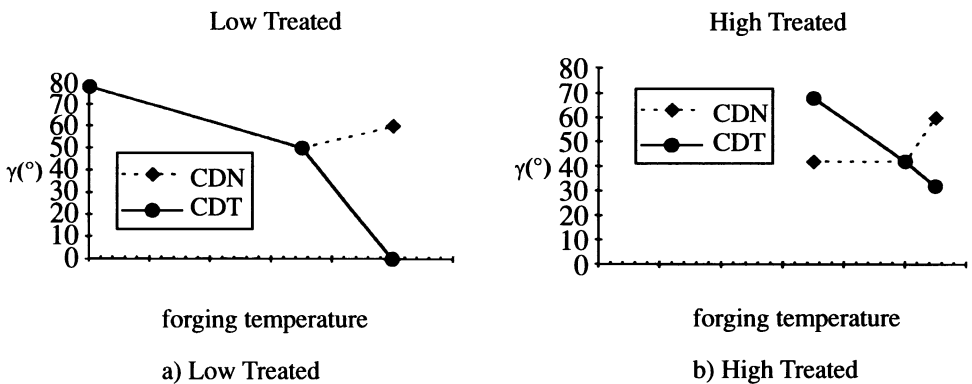


**Figure 6** Evolution of angle  $\gamma$ , between the axes  $\langle 0001 \rangle$  and the deformation axis D, with the forging temperature.

- The process with a deformation in the  $\beta$ -field leads to an acicular microstructure with different textures.

The forging or the unidirectional rolling leads to an acicular microstructure with a near basal/transverse texture.

On the contrary, the cross-rolling leads to an acicular microstructure with a basal texture.

- the forging process leads to two texture components with several microstructures bimodal or acicular. A bimodal microstructure is obtained after forging in high ( $\alpha + \beta$ ) phase field and an acicular microstructure in  $\beta$  phase field.

## CONCLUSION

\*The different deformation temperatures give three types of microstructure: equiaxed, acicular and bimodal. The solutioning temperature modifies the proportion of the different phases. A treatment at high temperature in the ( $\alpha + \beta$ ) field results in microstructures containing amounts of both primary  $\alpha$  phase and transformed  $\beta$  phase, less than a treatment at low temperature for which the  $\beta$  phase is stable in small proportion at the end of process.

\*In the present alloy, the typical textures obtained after different types of deformation are:

1. All the samples present a texture with two components  $C_{DN}$  and  $C_{DT}$ . The first  $C_{DN}$  corresponds to a single crystal with axis  $c$  contained in (D, N) plane of the specimen. The second  $C_{DT}$  corresponds to a single crystal with axis  $c$  contained in (D, T) plane.
2. The low solutioning treatment performed after the thermomechanical treatment does not change the texture. At the opposite, for the high solutioning treatment, the  $C_{DN}$  component is near to the basal texture and the  $C_{DT}$  is near to  $\{1010\}\langle 0001 \rangle$ .
3. These components evolve in opposite way both in intensity and in variation of the angle  $\gamma$  with the deformation temperature. At high temperature, the  $C_{DN}$  component is predominant and corresponds to the transverse texture  $\{1010\}\langle 1210 \rangle$ . At low temperature the reverse is observed with the tendency of  $C_{DT}$  to be parallel to the  $\{1010\}\langle 0001 \rangle$  texture.

## References

- Benhaddad, S. (1992). Thèse Doctorat Université Paris, XI.
- Bowen, A. W. (1988). 6th World Conference on Titanium, (ed. Lacombe, P., Tricot, R. and Béranger, G.), *Cannes*, 93.
- Bunge, H. J. (1969). *Mathematische Methoden der Texturanalyse*, Akademie Verlag, Berlin.
- Peters, M. and Lütjering, G. (1980). *Titanium Science and Technology*, (ed. Kimura, H. and Izumi, O.), Tokyo, 925.
- Roe, R. J. (1965). *Journal of Applied Physics*, **36**, 2024.
- Wanhill, R. J. H. (1978). 5th International Conference on Textures of Materials, (ed. Gottstein, G. and Lücke, K.), Springer Verlag, Aachen, 529.